LESM: a laser-driven sub-MeV electron source delivering ultra-high dose rate on thin biological samples

L Labate[1,7], M G Andreassi[2], F Baffigi[1], R Bizzarri[3], A Borghini[2], G C Bussolino[1], L Fulgentini[1], F Ghetti[3], A Giulietti[1], P Köster[1], D Lamia[4], T Levato[5], Y Oishi[6], S Pulignani[2], G Russo[4], A Sgarbossa[3] and L A Gizzi[1,7]

[1] Istituto Nazionale di Ottica, Consiglio Nazionale delle Ricerche, Pisa, Italy
[2] Istituto di Fisiologia Clinica, Consiglio Nazionale delle Ricerche, Pisa, Italy
[3] NEST, Istituto Nanoscienze, Consiglio Nazionale delle Ricerche and Scuola Normale Superiore, Pisa, Italy
[4] Istituto di Bioimmagini e Fisiologia Molecolare, Consiglio Nazionale delle Ricerche—LATO, Cefalù, Italy
[5] ELI-Beamlines, Institute of Physics of the Czech Academy of Science, Prague, Czech Republic
[6] Central Research Institute of Electric Power Industry, Kanagawa, Japan

E-mail: luca.labate@ino.it

Received 25 August 2015, revised 28 April 2016
Accepted for publication 12 May 2016
Published 14 June 2016

Abstract

We present a laser-driven source of electron bunches with average energy 260 keV and picosecond duration, which has been setup for radiobiological tests covering the previously untested sub-MeV energy range. Each bunch combines high charge with short duration and sub-millimeter range into a record instantaneous dose rate, as high as 10^9 Gy s^{-1}. The source can be operated at 10 Hz and its average dose rate is 35 mGy s^{-1}. Both the high instantaneous dose rate and high level of relative biological effectiveness, attached to sub-MeV electrons, make this source very attractive for studies of ultrafast radiobiology on thin cell samples. The source reliability, in terms of shot-to-shot stability of features such as mean energy, bunch charge and transverse beam profile, is discussed, along with a dosimetric characterization. Finally, a few preliminary biological tests performed with this source are presented.

Keywords: laser-driven electron accelerators, sub-MeV electron sources, ultrahigh dose rate, radiobiology, cell radiation damage

(Some figures may appear in colour only in the online journal)

1. Introduction

Ionizing radiation penetrating biological materials deposits its energy by means of ionization and excitation of molecules and atoms in the material. Different types of radiation produce different patterns of energy deposition through the matter, depending on mass and energy of the particle (or photon) and the physical and chemical properties of the stopping medium [1, 2].

The fundamental quantity to relate radiation effects to biology is the absorbed dose. The relative biological effectiveness (RBE) of a radiation is the ratio between the degree of damage induced by this radiation for a given biological endpoint at given dose and the damage induced with the same absorbed dose by the reference radiation (usually 220 kVp x-rays or ^{60}Co γ photons). RBE values have been obtained from experimental data and model calculations for a variety of biological endpoints such as cell death, chromosome aberration, micronuclei formation and induction of single- and double-strand breaks (SSB and DSB from now on, respectively).

The biological effects of ionizing radiation, however, cannot be explained as a sole function of the dose. Other quantities

[7] Also at Istituto Nazionale di Fisica Nucleare, Sezione di Pisa, Italy.

such as linear energy transfer (LET), radiation quality and, more recently, track structure and microdosimetry have been used to provide a deeper understanding of biological effects leading to a given radiation effectiveness [3]. For instance, epidemiological and experimental analysis indicates that low-LET radiations (x-rays, electrons) seem to have different RBEs depending on their energy, so that higher energy radiation can be relatively less effective than lower energy one. For instance, there is a factor of about 3–6 increase in effectiveness for tritium beta rays (electrons of a few KeV kinetic energy) compared to 15 MeV electrons [4]. Such an example highlights the importance of the availability of low-energy electron sources, even, as will be clear in the following, at ultrahigh dose rates.

Several studies have been carried out in order to assess the RBE of low energy electrons from conventional sources (in this work we call conventional all but laser-driven sources). Folkard *et al* [5] experimentally ascertained the fraction of DNA single- and double-strand breaks induced by mono-energetic electrons in the range 25–4000 eV produced by an electron gun, showing that single energy deposition of no more than 50 eV within dehydrated DNA is sufficient to induce a DSB. Beside experimental results, the most complete approach to describe RBE of electrons lies on track structure calculations by means of Monte Carlo simulations, which are capable of simulating and recording the energy transferred by every single particle in each interaction, and to determine and register its energy deposition in the medium. Such calculations have been reported for electrons and ultrasoft x-rays by Nikjoo and co-workers [6, 7], showing that while sparsely ionising components of 100 keV electrons tracks predominate, the contribution from lower energy secondary electrons (leading to the larger energy deposition) is also relevant.

Hsiao and Stewart [8] used the Monte Carlo radiation transport code PENELOPE to estimate the spectrum of initial electrons and combine this information with DNA damage yields for monoenergetic electrons from a previous study [9] to obtain nucleotide-level maps of clustered DNA lesions including single and double strand breaks. Goodhead [10, 11] examined the complexity of DNA damage induced by ionizing tracks of different shape and size and concluded some general and specific features of cellular responses to ionizing radiation.

This very stimulating scientific scenario has been further enriched by the availability of high energy particles provided by plasma accelerators driven by ultra-short intense laser pulses. In fact, innovative aspects of radiation biology are rapidly growing as a result of novel electron and ion sources based on laser-driven acceleration, providing ultra-short (picosecond or sub-picosecond) particle bunches [12]. As a consequence, it appears that new physical concepts on radiation interaction with living matter have to be considered, taking into account the extremely high peak dose delivered [13–16].

Since our work is devoted to energetic electron sources, let's briefly mention that laser-driven electron acceleration in plasmas (based upon the so-called Laser WakeField Acceleration process, LWFA from now on), after the original proposal by Tajima and Dawson in 1979 [17], has experienced an outstanding development in the last decade, mainly due to the increasing availability of table-top, multi-terawatt, femtosecond-pulse CPA laser systems. Laser plasma accelerators are now capable of delivering ultrashort (on the time scale of molecular motions [18, 19]) high energy electron bunches that open up exciting perspectives, especially for biochemical and biophysical domains. Indeed, the complex links existing between the physical aspects of early energy deposition events and the delayed evolution to biological endpoints is a matter of intense investigation and it can greatly take advantage of the availability of ultrashort sources [14, 20].

Laser-plasma acceleration originates from the unique properties of plasma to support electric fields exceeding 100 GV m^{-1}, orders of magnitude higher than the 10–100 MV m^{-1} supported by radio-frequency cavities of conventional accelerators [21, 22]. The generation of such large electric fields is ordinarily achieved by focusing an ultra-short and multi-TW laser pulse onto a gas target, tipically a supersonic gas jet. The ultrashort bunch duration of laser-driven electron sources leads to 10^6–10^8 times higher instantaneous dose rates than in typical electron gun or LINAC counterparts (when no bunch compression schemes are used). For instance, a typical electron accelerator for internal radiotherapy currently deliver from 0.1 up to 10 cGy per pulse, with typical bunch duration of the order of a few microseconds, leading to an instantaneous dose rate of $\sim 10^3$–10^5 Gy s^{-1} (see, for instance, [23]). On the other hand, a laser-plasma source can deliver $\sim$1–10 mGy per pulse, with a characteristic 0.1–1 ps duration (see, for instance, [24–26]); these values lead to instantaneous dose rates $\sim 10^9$–10^{11} Gy s^{-1}. Furthermore, considering the typical LINACs and ultrashort laser systems repetition rates, the average dose can be potentially comparable. This has spawn an intense research activity aimed at demonstrating medical applications. For instance, recently, Beyreuther *et al* [24] have shown the general applicability of laser accelerated electrons for *in vitro* cell experimentation, while Laschinsky *et al* [27] irradiated tumour and non-malignant cells with pulsed laser accelerated electrons for the comparison with continuous electrons of a conventional therapy LINAC.

Previous works on biomedical use of laser-driven acceleration, however, were mostly focused on possible future application of laser accelerated particles to radiotherapy, with the production of particles with energies from a few up to a few tens of MeV. So far, no investigations have been carried out on the effects of laser accelerated lower energy (from 0.1 to 1 MeV) electrons on biological samples. In this energy range, as a matter of fact, both DC and pulsed solutions have been reported (and a couple of commercial solutions are available), based on conventional acceleration mechanisms. In [28] an electron source based on an electron gun and operating in the range 160–200 keV was presented, featuring a large enough (200×100 mm^2) exit window to be used for applications in medicine and material science. This device was able to operate at a rep rate of 50 Hz. The bunch duration was 5 μs.

Given the interest in ultrashort electron sources in this 'low' energy range, several proposals and/or experimental studies have been published in the past few years, which used an ultrashort laser beam as the driver. These studies aimed,

in particular, at ultrafast electron diffraction (UED) as the main application. In particular, He *et al* [29, 30] reported on the use of a few mJ ultrashort laser pulse to generate ~100 keV electron bunches via LWFA. In this case, the total charge per bunch was of the order of 10 fC. Recently, a 240 keV ultrashort electron source was studied numerically, using PIC simulations, based on the Direct Laser Acceleration scheme in a gas [31]. It is also worth to note that ultrashort electron bunches can be obtained using conventional techniques, provided that advanced bunch compression schemes are used, although this schemes are in general best suited for relativistic electron beams (see for instance [32] and [33]).

In this paper, we report on the performances and preliminary biology experiments of a LWFA source (dubbed 'LESM: laser-driven electron source in the sub-MeV range') in the 100–300 keV energy range. In contrast to the above mentioned ultrashort sources, delivering ~10 fC to ~1 pC bunches and targeting the UED as the main application, our source delivers ~100 pC bunches and is best suited for experiments in radiobiology, allowing an irradiation of a few centimeters wide biological samples. As a matter of fact, as reviewed in [3], the ~100 keV electron energy range deserves a great interest in biology. Together with the sub-picosecond bunch duration, the above figures for our source result in an unprecedented instantanous dose rate, of the order of 10^9 Gy s^{-1}, of high-RBE ionizing radiation. This device is very attractive for biophysical investigations, such as induction of localized radical processes and their amplification up to mutagenic DNA lesions and protein impairment, to our knowledge never performed before with electron bunches of such an energy and at such an extreme dose-rate. Preliminary results of such radiobiological studies are reported in the last section. Other noteworthy features of our source, such as its use for electron radiography [34] and the focusability of the electron bunch [35] to locally enhance the dose deposition, have been reported elsewhere and will not be discussed here.

2. The laser-driven electron source

The electron source was designed, set-up, tuned and tested at the Intense Laser Irradiation Laboratory (ILIL) of the National Institute of Optics of CNR in Pisa (Italy), using a laser system operating at 2 TW power level. The 10 Hz, 800 nm Ti:sapphire laser delivered 40 fs pulses of 80 mJ energy and featured an ASE (Amplified Spontaneous Emission) contrast ratio $>10^7$. The laser beam was focused with an *f*/5 off-axis parabolic (OAP) mirror down to a 10 μm diameter spot (containing >50% of the pulse energy) into a supersonic nitrogen (N_2) gas-jet delivered by a rectangular nozzle 4 × 1.2 mm in size (the laser propagated along the smaller side, see figure 1); the corresponding nominal laser intensity in the waist was then $\sim 1.3 \times 10^{18}$ W cm^{-2}. The laser-plasma interaction was diagnosed using standard techniques such as optical (Nomarski) interferometry and Thomson scattering imaging. The density distribution in the jet (for both neutral gas and plasma) was measured by interferometry and used to tune numerical simulations, as detailed below.

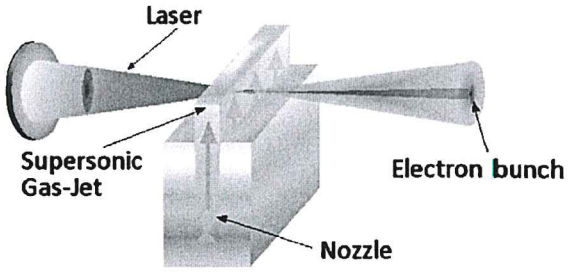

Figure 1. Conceptual layout of the laser-driven electron accelerator.

A scan of the gas backing pressure and of the laser beam waist position along the gas-jet was performed in order to get the best suitable conditions for the electron acceleration. Nevertheless, a tuning of the ASE contrast ratio was needed in our case to find a stable accelerating regime; in the rest of this section a brief glance at our acceleration regime will be given, although a deeper discussion is outside the scope of this paper and will be presented elsewhere. Due to the limited maximum intensity on target, lower than the expected threshold for self-injection (see [36] and references therein), a rather high backing pressure $P_{\text{backing}} \simeq 40$ bar (corresponding to an electron density well in excess of 10^{20} cm^{-3}) was first used in our case to get trapped and accelerated electrons with the optimal contrast ratio given above. Indeed, as it is well known, the threshold for self-focusing is easily achieved at these high densities, allowing an enhancement of the intensity to be reached within the plasma [37]. However, in this condition the acceleration regime exhibited a rather poor stability ($\lesssim$20% shot with an accelerated bunch). A much more stable condition was found working at a lower backing pressure $P_{\text{backing}} \simeq 15$ bar (corresponding to a maximum electron density $n_e \simeq 5 \times 10^{19}$ cm^{-3}) and introducing a pre-plasma by degrading the ASE contrast ratio. Indeed, by acting on the Pockels cells delay in the regen amplifier, the contrast ratio was reduced down to $\sim 10^6$, measured 3 ns before the main pulse. With this contrast, the ASE reached an intensity of about 10^{12} W cm^{-2}, well above the breakdown threshold for the gas. In previous experiments reported in the literature, a low contrast ratio, either at the ns or at the ps level, was employed in order to create a plasma channel able to guide the main pulse and possibly reducing the energy spread [38] and/or leading to a spatial cleaning of the main pulse itself [39]. In our case, where a rather low laser intensity was available, this low contrast regime led to a much more reliable acceleration regime, with $\gtrsim$90% shots providing an accelerated bunch. This was attributed to an enhanced trapping, similar to the one described in [40], at the entrance of the pre-plasma region, where a density downramp is found. Indeed, according to hydrodynamic simulations performed with the code POLLUX [41], whose predictions were matched and compared to our density measurements, a pre-plasma was created in these conditions, with a temperature of a few tens of eV and an ionization degree of about 3–4. Due to the hydrodynamic expansion, this pre-plasma was found to exhibit a rather pronounced density downramp at its entrance at the time of the arrival of the main pulse. In particular, the local electron density decreases of

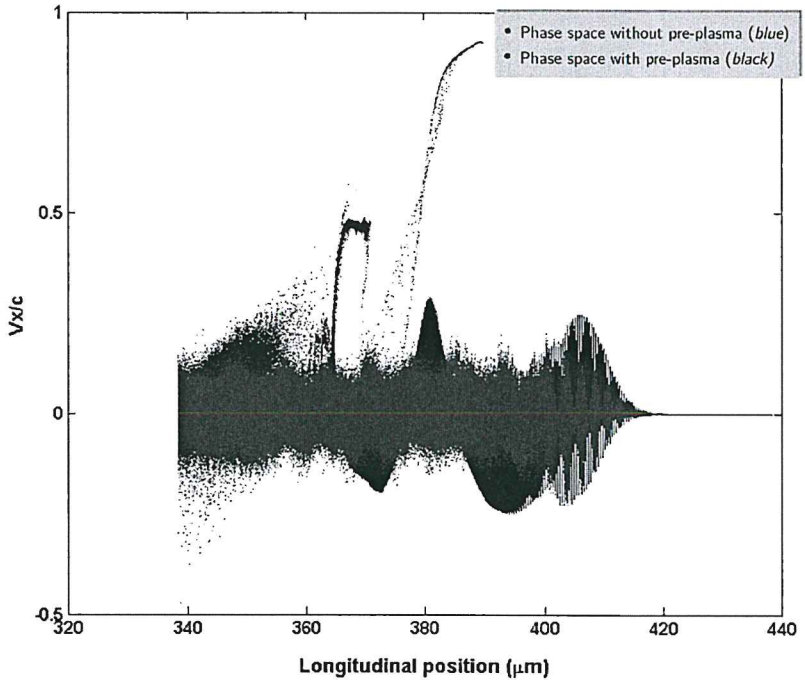

Figure 2. Comparison of the longitudinal phase space provided by a PIC simulation with and without preplasma.

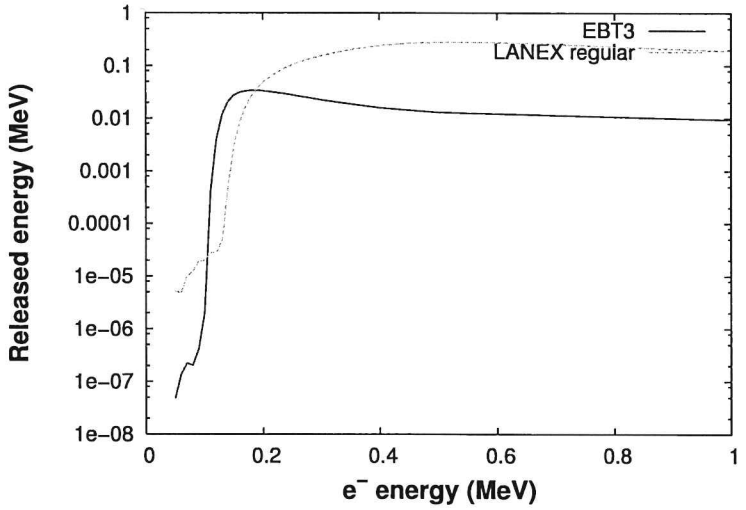

Figure 3. Energy released by an electron into the sensitive layer of an EBT3 gafchromic film and on a LANEX scintillator screen as a function of its initial energy, as retrieved by Monte Carlo simulations.

one order of magnitude, from the maximum value of about 5×10^{19} cm^{-3}, over a few plasma wavelengths. The observed enhancement of the trapping process was qualitatively confirmed by 2D particle-in-cell (PIC) simulations, carried out using the EPOCH code [42]. The initial electron density profile was gained by the POLLUX simulations. Figure 2 shows a snapshot of the longitudinal phase space at the time of the maximum acceleration in the two cases in which a pre-plasma with a density downramp is present or an initial flat density profile is assumed. As it appears, no accelerated electrons are observed in the absence of the pre-plasma. In contrast, electrons with a calculated average energy of ~300 keV are observed when a pre-plasma is present.

From the experimental point of view, a remarkable improvement of the shot-to-shot stability of our source was observed in this case; indeed, this led to a dramatic increase of the percentage of shots producing an accelerated bunch, from $\lesssim$20% up to $\gtrsim$90%.

3. Characterization of the electron bunch for applications in radiobiology

3.1. Study of the electron bunch parameters

The electron spectrum was obtained using a magnetic spectrometer equipped with a 0.5″ long (in the electron beam

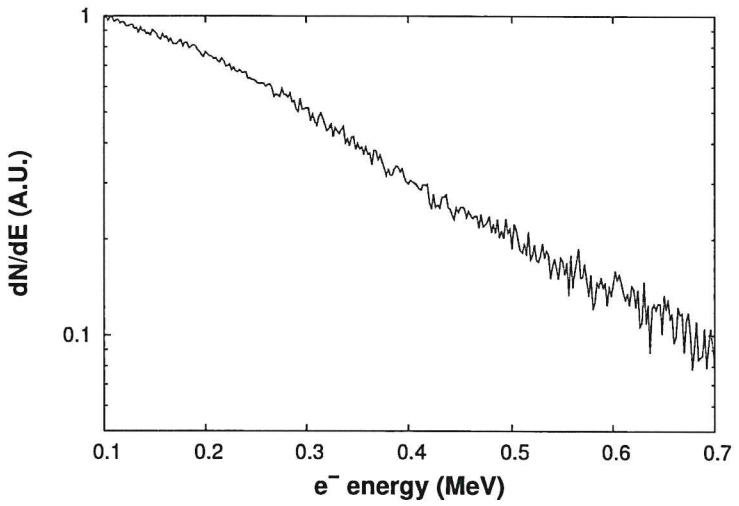

Figure 4. Electron energy spectrum measured using a magnetic spectrometer.

direction) permanent magnets dipole providing a 0.2 T magnetic field. A 0.5 mm width slit (made on a lead substrate) was used in front of the dipole. The energy resolution, retrieved taking into account the spectrometer geometry, the bunch divergence and the detector resolution, was estimated to be $\delta E/E \lesssim 5 \times 10^{-2}$. A Kodak LANEX (type 'regular') scintillator screen imaged out by an optical camera was used as a detector. Figure 3 shows the sensitivity of the LANEX screen as obtained by Monte Carlo simulations of the energy deposition carried out using the GEANT4 library toolkit [43]. It should be pointed out that both our magnetic dipole and the LANEX screen allowed electrons with an energy $\gtrsim 100$ keV to be detected. A typical electron spectrum, obtained from a single shot, is shown in figure 4. The curve can be fitted with an exponential function with mean energy $\bar{E} \simeq 260$ keV, which is in a reasonable agreement with the value retrieved by the PIC simulations given above. Furthermore, we have observed fluctuations of the order of 10% r.m.s. in this value when averaging over a large number (a few hundreds) of shots. This r.m.s. value was obtained considering only the shots for which an electron signal was observed, which, we remind, were a fraction of about 90% of the total laser shots.

The electron bunch divergence and charge were retrieved using the so-called SHEEBA detector [44]. It basically consists of a stack of gafchromic films and suitable electron attenuators. The main electron bunch parameters, such as the spectrum, divergence and total charge can be retrieved, using an iterative algorithm, by the measured change of the optical density occurring on each gafchromic layer due to the electron energy deposition. In our case, EBT3 type gafchromic films were used. Figure 3 shows the energy released into the sensitive layer of an EBT3 film as a function of the impinging electron energy, as retrieved by GEANT4-based Monte Carlo simulations. We used such a kind of simulation, along with both numerical and experimental measurements of the EBT3 dose response curves (see [45] for further details) to get an absolute calibration of the EBT3 sensitivity as a function of the electron energy. As clearly visible from the plot, a noticeable dependence of the energy released by each electron upon its initial energy occurs in the energy range of our source. This dependence is taken into account in our analysis algorithm. It is worth noting, at this point, that although a departure of the actual (that is, measured) sensitivity of EBT3 films from the one retrieved using Monte Carlo simulations has been reported for protons [46], this is expected to occur at a negligible level in the electron case. Indeed, this departure can be attributed to the finite number density of the molecules whose polymerization is responsible for the observable darkening of the EBT3 films; this finite density may lead to a saturation in the case of high LET particles, as the energy release occurs on a very thin layer. As a matter of fact, this effect has been observed mostly with low energy (a few MeV) protons, exhibiting a high LET, while no discrepancy between simulated and measured response was reported for electrons (see, for instance, [47]).

As said above. the effective energy released by each electron onto the gafchromic sensitive layer is taken into account by the SHEEBA detector analysis algorithm (see [44] for further details); this is particularly important in view of the strong variations of the EBT3 sensitivity across the energy range of interest in this work.

Each measurements using the SHEEBA detector was integrated over 50 laser shots. Table 1 shows, along with other relevant figures for our source, the measured bunch divergence and the total charge per bunch. As it appears, the bunch has a divergence of about 20° FWHM; this allows biological samples with a transverse extent of a few centimeters to be irradiated; this issue will be discussed below. Furthermore, the pretty high charge per bunch as compared to similar laser-driven sources allows doses of a few tens of mGy s^{-1} to be delivered. Both these issues will be deepened below.

Finally, we mention here that the SHEEBA detector is also able to provide an independent measurement of the electron spectrum, although with a lower energy resolution with respect to a magnetic spectrometer, without the need of any assumption on the shape of the electron spectrum. This feature was used as a cross-check of the measurements performed with the magnetic spectrometer and provided an estimate of

Table 1. Main features of the source.

Paramater	Value
Electron average energy	260 keV
Spectral shape	exponential
Bunch divergence	20° FWHM
Bunch charge	$\gtrsim$100 pC
Repetition rate	up to 10 Hz
Bunch duration on the sample	3.5 ps
Peak current	>100 A
Non-uniformity on sample	<10% (over 25 shots)
Stopping power in water	2.49 MeV cm^2 g^{-1}
Range in water	0.68 mm
Dose per pulse	3.5 $\pm$ 7% mGy
Peak dose rate	10^9 Gy s^{-1}
Average dose rate	35 mGy s^{-1}

the spectral shape and mean energy in agreement with those given above.

3.2. Experimental setup and dosimetry for radiobiology experiments

In order to allow the irradiation in air of biological samples, the experimental setup used is shown in figure 5. The laser beam enters the vacuum chamber from the left and is focused in the gas jet by the OAP (see section 2 for details). In order to put the living sample in air as close as possible ($\sim$10 cm) to the divergent electron source, we modified one of the vacuum chamber flange as shown in figure 5 in order to allow the insertion of a tube, ending with a window for electrons, through the modified flange. A 50 μm thick plastic (kapton) window with a clear aperture of 25 mm was used as a vacuum-air interface. Ad hoc plastic holders, one for each type of dishes used (Petri dishes and Corning cell culture flasks, in the cases discussed in the next section), were built in order to allow a precise (within $\sim$0.5 mm) insertion and positioning of the samples into the tube. The holders also allowed a precise positioning of the gafchromic films which were used to get the effective dose on each sample (see below). The biological samples were inserted into the tube up to a few millimeters distance from the window, at a total distance of about 12 cm from the electron source.

The electron propagation in vacuum, across the window and in air up to the sample position was simulated using a code based on the Monte Carlo GEANT4 library toolkit [43]. In particular, the simulated setup included the gas-jet structure, the vacuum chamber, the start and end flanges of the inserted tube, the tube itself and the plastic window. In the simulations, the low-energy *LowEm_Penelope* physics model was used [48]; this package (and the related cross sections database) allows interaction processes (including Compton scattering, photoelectric effect, Rayleigh scattering, gamma conversion, Bremsstrahlung, ionization and positron annihilation) occurring at energies down to 250 eV to be taken into account.

Figure 6 shows the distribution of the arrival times of the electrons at the sample position as gathered from the simulation. In the simulation (where no account was made of Coulomb bunch lengthening) all the primary electrons were considered to leave the gas-jet at the same time ($t = 0$). Thus the curve shown would actually have to be considered as a transfer curve to be convolved with the actual bunch duration in order to get the final bunch time profile. However, as it is well known, durations of a few up to a few tens of femtoseconds have been reported for the bunches on leaving the plasma (see for instance [49]); this means that, looking at the figure, a bunch duration of a few picoseconds can be safely estimated/calculated at the position of the biological samples. This duration is still about six orders of magnitude smaller than that of a typical electron gun or LINAC (when no advanced bunch compression schemes are used [32, 33]).

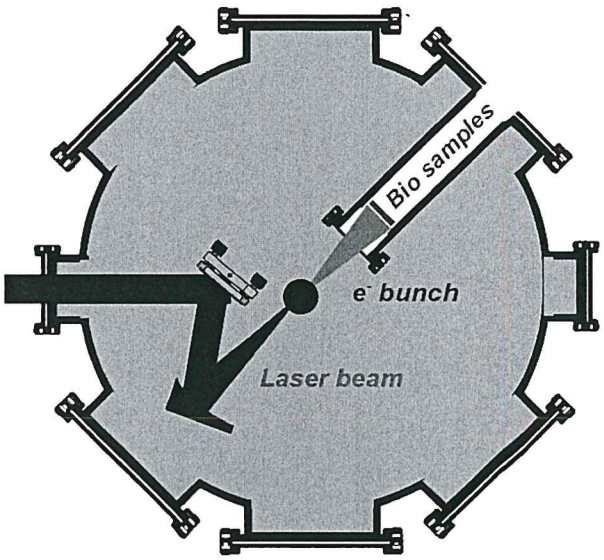

Figure 5. Layout of the experimental setup for the irradiation of biological samples.

GEANT4 simulations also confirmed that the energy spectrum of the electrons reaching the sample is basically the same as measured in vacuum, namely an exponential spectrum with mean energy $\bar{E} \simeq 260$ keV.

The transverse profile of the electron beam at the sample position was measured using a LANEX screen imaged out by a CCD camera. On each shot, the beam exhibited, across the 25 mm window aperture, large scale (scalelength comparable to the aperture) variations of about 5%, with occasional 'hot spots' (with typical size of a few millimeters) where the beam intensity was from 10 up to 15% higher than the average intensity. Both the large scale non-uniformities and the hot spots showed a random position, so that the tranverse beam intensity profile could be considered uniform within a few percent when a few tens of shots (corresponding to a few tens of mGy, as it will be shown in a moment) were accumulated on the sample.

An experimental measurement of the dose delivered by our source was also carried out. In particular, a stack of EBT3 films separated by sheets of water-equivalent RW3 material (PTW, Freiburg) was placed at the position of the sample, that is inside the tube shown in the figure. The dose was then

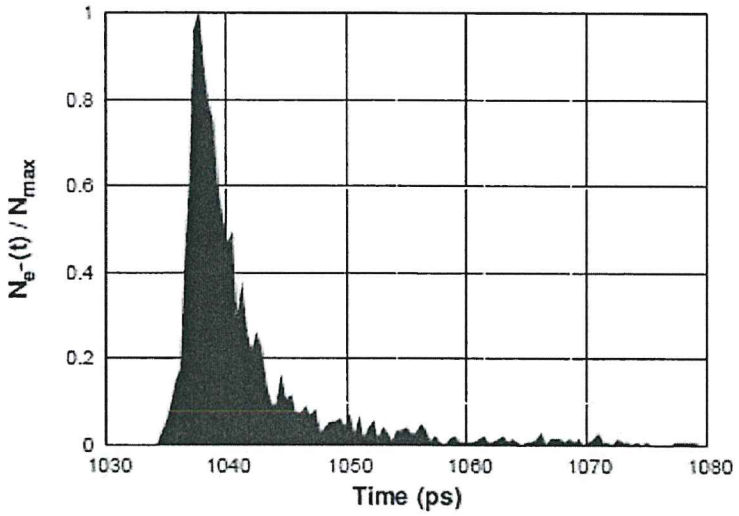

Figure 6. Distribution of the arrival times of the electrons at the sample position, as retrieved by Monte Carlo simulations.

retrieved by comparing the experimental measurements with the predictions of Monte Carlo simulations (based again on the GEANT4 library toolkit). Further details on the entire procedure, which also involved preliminary dose-response calibration of each EBT3 film using a conventional electron source, can be found in [45]. Each measurement was carried out by integrating over 50 laser shots. The dose delivered to the samples (integrated over the whole 25 mm aperture) measured in this way was $D = 3.5 \pm 7\%$ mGy shot^{-1}. This value includes the contamination due to Bremsstrahlung photons, whose contribution was estimated, using the Monte Carlo simulations, to be $\lesssim 1\%$.

Finally, we point out that the effective dose delivered to each biological sample in the biology tests briefly discussed below was monitored by using layers of EBT3 film placed both upstream and downstream of each sample dish and comparing the measured absorbed dose with the predictions of our Monte Carlo code.

4. Preliminary radiobiological tests

The biological effectiveness of the LESM source has been preliminarily tested with conventional radiobiological assays, such as γ-H2AX foci assay on human lymphocites and FRAP analysis of the alterations in the biochemical mechanisms regulating the nucleocytoplasmic translocation in CHO (Chinese hamster ovary) cells. DNA double-strand breaks (DSB) are a major DNA damage and a key mechanism through which radiotherapy and some chemotherapeutic agents kill cancer cells [50]. Nuclear γ-H2AX foci represent a marker for DSB formation and the first detectable response of cells to DSBs [51]. DSBs can be identified *in situ* by detecting the γ-H2AX foci formed at DNA break sites utilizing immunostaining techniques, making the γ-H2AX foci assay the most sensitive of current assays for irradiation-induced DSBs [52]. Recently, proof-of-principle experiments with accelerators of protons or electrons have been performed showing that beams are able to generate DNA damage [53–55]. We used the γ-H2AX foci assay to measure DSBs induced by our electron source on human lymphocytes, irradiating our samples with different numbers of cumulated laser shots in order to assess DNA damage at different doses.

Figure 7 shows the results of a test in which lymphocytes were irradiated with effective doses of 75, 155 and 315 mGy (the cells were fixed after 1 h). On the left, the number of γ-H2AX foci per cell as a function of the absorbed dose is shown (this value was measured at 30 min time after the fixation). Given that on average 0.2–0.4 foci are induced per 10 mGy per cell when using LINAC electrons [50, 51], this would suggest, if the ultrashort nature of the source had no effect on the observed damage, an absorbed dose comparable to the one actually delivered with our source. For the sake of completeness, the residual DNA DSBs at different times corresponding to an absorbed dose of 155 mGy are shown on the right.

A different assay was carried out in order to evaluate the possible effects of the electron bunches on the biochemical mechanisms regulating nucleocytoplasmic translocation (and thereby protein/RNA shuttling at intracellular level) in standard CHO cells. This kind of test is particulary relevant for the studies of low dose radiation damages. To do this, we took advantage of an established translocation model based on the fusion construct between enhanced fluorescent protein and the nuclear localization sequence of SV40 (NLS-EGFP) [56]. The nucleocytoplasmic translocation rates of this construct can be easily obtained by a previously published experimental approach involving the fluorescence recovery after photobleaching technique [57]. More specifically, we exposed CHO cells transiently expressing NLS-EGFP to LESM electrons and we evaluated the modifications in the translocation time (τ) and permeability to passive diffusion (P) as compared to a set of non-exposed cells. Data analysis yielded translocation time $\langle\tau\rangle = 135 \pm 69$ s for control cells (#10 cells) and $\langle\tau\rangle = 152 \pm 97$ s (#14 cells) for irradiated cells, with a T-test ($p = 0.64$) indicating that the differences between the two data sets were not statistically significant. As for the passive permeability, data analysis yielded $P = 7.5 \pm 5.7$ μm^3 s^{-1} for

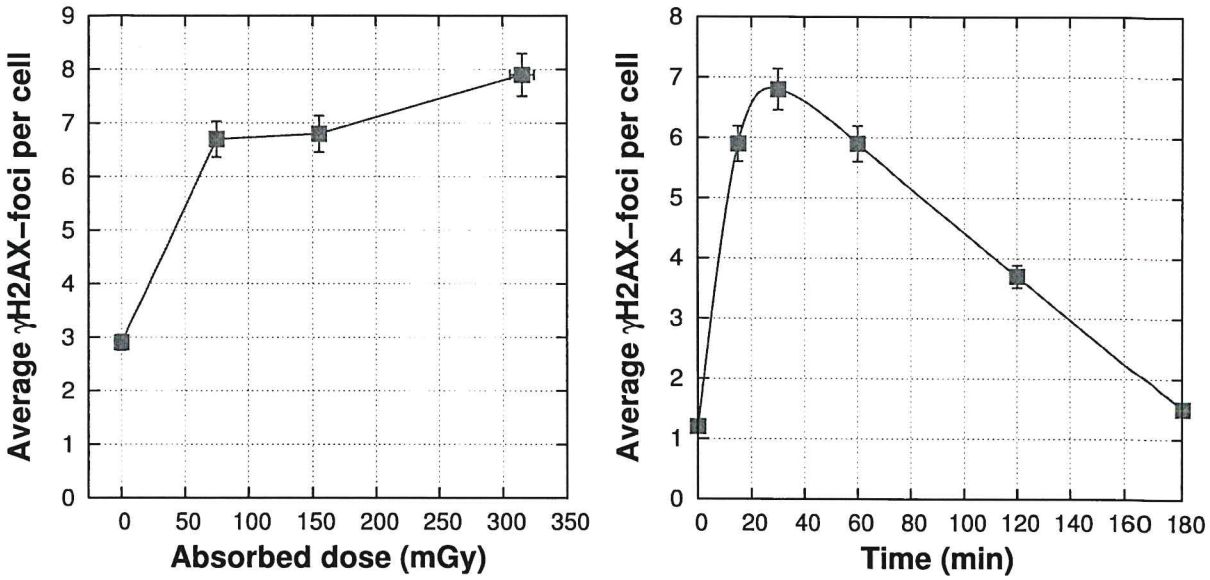

Figure 7. *(left)*: Average number of γ-H2AX foci per cell as a function of the absorbed dose. *(right)*: Average number of γ-H2AX foci per cell at different times corresponding to an absorbed dose of 155 mGy; this quantity is related to the cell ability to repair the DNA over successive divisions. The error on the measurements of the number of foci is $\pm 5\%$ and the error on the measured effective dose is $\pm 3\%$.

control cells and $P = 5.7 \pm 3.3\ \mu m^3\ s^{-1}$ for irradiated cells, again showing the negligible differences between the two data sets (T-test afforded $p = 0.4$). This preliminary analysis seems to suggest that irradiation with LESM electrons do not affect this particular biochemical mechanisms.

5. Summary and conclusions

We reported on an ultrashort laser-driven electron source for experiments in biology with sub-MeV electron beams. The source, which is based on the interaction of a relatively low power (2 TW) ultrashort laser system with a gas-jet, is suitable for measurements (so far unreported) of the RBE of sub-relativistic electrons at ultrahigh instantaneous dose rates. The laser-plasma source was equipped with a vacuum-air interface in order to allow irradiation of *in vitro* biological samples. A full dosimetric characterization was performed, using standard dosimetric techniques, comparing experimental measurements to Monte Carlo simulations. LESM can deliver a dose of about 3.5 mGy per shot at the sample position. In order to assess the capability of our new source, different human cells (namely, lymphocytes, fibroblasts) and CHO (Chinese Hamster Ovary) cells have been irradiated and the induced biological effects in terms of cellular DNA damage and alteration of biochemical mechanisms have been studied by means of well-established biological techniques (scoring of γ-H2AX, FRAP). In particular, our experiments showed DNA double strand breaks levels similar to the one induced by conventional electron beams, while no appreciable alteration was found affecting the biochemical mechanisms that regulate the nucleocytoplasmic translocation. The noteworthy stability and the ultrashort bunch duration make this source very appealing for many experimental tests of interest in sub-MeV electron damage biology.

Acknowledgments

The activity of the INO-CNR Pisa group was partially supported from the Italian Ministry of Health through the Project No. GR-2009-1608935 (Study of Radiobiological and Radiotherapic Effects of a Novel Laser-Driven Electron Accelerator, D.I. AgeNaS), from the CNR funded Italian research Network ELI-Italy (Attoseconds) and from the PRIN project (Contract No. PRIN2012AY5LEL). The Pisa authors also acknowledge contribution from the MIUR-FIRB project SPARX (Sorgente Pulsata Auto-Amplificata di Radiazione X) and the INFN gResist and Plasma-med collaborations.

References

[1] Carron N J 2006 *An Introduction to the Passage of Energetic Particles Through Matter* (Boca Raton, FL: CRC Press)
[2] Lindborg L and Nikjoo H 2011 *Radiat. Prot. Dosim.* **143** 402
[3] Nikjoo H and Lindborg L 2010 *Phys. Med. Biol.* **55** R65
[4] Hunter N and Muirhead C R 2009 *J. Radiol. Prot.* **29** 5
[5] Folkard M, Prise K M, Vojnovic B, Davies S, Roper M J and Michael B D 1993 *Int. J. Radiat. Biol.* **64** 651
[6] Nikjoo H, Goodhead D T, Charlton D E and Paretzke H G 1989 *Phys. Med. Biol.* **34** 691
[7] Nikjoo H, Bolton C E, Watanabe R, Terrissol M, O'Neill P and Goodhead D T 2002 *Radiat. Prot. Dosim.* **99** 77
[8] Hsiao Y and Stewart R D 2008 *Phys. Med. Biol.* **53** 233
[9] Semenenko V A and Stewart R D 2006 *Phys. Med. Biol.* **51** 1693
[10] Goodhead D T 1992 Track structure considerations in low dose and low dose rate effects of ionizing radiation *Effects of Low Dose and Low Dose Rate Radiation* (*Advances in Radiation Biology* vol 16) ed O F Nygaard *et al* (London: Academic)
[11] Goodhead D T 1994 *Int. J. Radiat. Biol.* **65** 7

[12] Giulietti A, Bussolino G, Fulgentini L, Koester P, Labate L and Gizzi L A 2015 Laser-plasma particle sources for biology and medicine *Progress in Ultrafast Intense Laser Science XII* (*Springer Series in Chemical Physics* vol 112) ed K Yamanouchi *et al* (Heidelberg: Springer)
[13] Gauduel Y A, Lundh O, Martin M T and Malka V 2012 Laser-plasma accelerators-based high energy radiation femtochemistry and spatio-temporal radiation biomedicine *Proc. SPIE* **8433** 843316
[14] Malka V, Faure J and Gauduel Y A 2010 *Mut. Res. Rev.* **704** 142
[15] Tajima J, Habs D and Yan X 2009 *Rev. Accel. Sci. Technol.* **2** 201
[16] DesRosiers C, Moskin V and Minsong C 2008 Laser-plasma generated very high energy electrons in radiation therapy of the prostate *Proc. SPIE* **6881** 688109
[17] Tajima J and Dawson J M 1979 *Phys. Rev. Lett.* **43** 267
[18] Brozek-Pluska B, Gliger D, Hallou A, Malka V and Gauduel Y 2005 *Rad. Phys. Chem.* **72** 149
[19] Gauduel Y A 2008 Femtochemistry: lasers to investigate ultrafast reactions *Lasers in Chemistry* vol 2, ed T Lackner (New York: Wiley)
[20] Gauduel Y A 2012 *J. Phys.: Conf. Ser.* **373** 012012
[21] Malka V and Mora P 2009 *C. R. Phys.* **10** 106
[22] Esarey E, Schroeder C B and Leemans W P 2009 *Rev. Mod. Phys.* **81** 1229
[23] Righi S, Karaj E, Felici G and Di Martino F 2013 *J. Appl. Clin. Med. Phys.* **14** 6
[24] Beyreuther E *et al* 2010 *Med. Phys.* **37** 1392
[25] Lundh O, Rechatin C, Faure J, Ben-Ismaïl A, Lim J, De Wagter C, De Neve W, Malka V 2012 *Med. Phys.* **39** 3501
[26] Andreassi M G *et al* 2016 *Radiat. Res.* at press
[27] Laschinsky L *et al* 2012 *J. Radiat. Res.* **53** 395
[28] Bogdanovitch B, Senioukov V, Koroliov A and Simonov K 1999 *Proc. 1999 Particle Accelerator Conf. (New York)* vol 4 p 2570
[29] He Z H, Hou B, Nees J A, Easter J H, Faure J, Krushelnick K and Thomas A G R 2013 *New J. Phys.* **15** 053016
[30] He Z H, Thomas A G R, Beaurepaire B, Nees J A, Hou B, Malka V, Krushelnick K and Faure J 2013 *Appl. Phys. Lett.* **102** 064104
[31] Marceau V, Varin C, Brabec T and Pichè M 2013 *Phys. Rev. Lett.* **111** 224801
[32] Han J-H 2011 *Phys. Rev. Spec. Top. Accel. Beams* **14** 050101
[33] Nozawa I *et al* 2014 *Phys. Rev. Spec. Top. Accel. Beams* **17** 072803
[34] Bussolino G, Faenov A, Giulietti A, Giulietti D, Koester P, Labate L, Levato T, Pikuz T and Gizzi L A 2013 *J. Phys. D: Appl. Phys.* **46** 245501
[35] Oishi Y, Giulietti D, Baffigi F, Fulgentini L, Giulietti A, Koester P, Labate L, Kando M and Gizzi L A 2014 *Japan. J. Appl. Phys.* **53** 092702
[36] Benedetti C, Schroeder C B, Esarey E, Rossi F and Leemans W P 2013 *Phys. Plasmas* **20** 103108
[37] Pathak N C, Bussolino G, Cecchetti C A, Giulietti A, Giulietti D, Koester P, Levato T, Labate L and Gizzi L A 2012 *Nucl. Instrum. Methods Phys. Res.* A **680** 103
[38] Hosokai T *et al* 2006 *Phys. Rev.* E **73** 036407
[39] Giulietti A *et al* 2006 *Phys. Plasmas* **13** 093103
[40] Geddes C G R, Nakamura K, Plateau G R, Toth Cs, Cormier-Michel E, Esarey E, Schroeder C B, Cary J R and Leemans W P 2008 *Phys. Rev. Lett.* **100** 215004
[41] Pert G 1983 *J. Comput. Phys.* **49** 1
[42] Arber T D *et al* 2015 *Plasma Phys. Control. Fusion* **57** 113001
[43] Agostinelli S *et al* 2003 *Nucl. Instrum. Methods Phys. Res.* A **506** 250
[44] Galimberti M, Giulietti A, Giulietti D and Gizzi L A 2005 *Rev. Sci. Instrum.* **76** 053303
[45] Lamia D *et al* 2015 *Nucl. Instrum. Methods Phys. Res.* A **786** 113
[46] Kirby D, Green S, Palmans H, Hugtenburg R, Wojnecki C and Parker D 2010 *Phys. Med. Biol.* **55** 417
[47] Sipilä P, Ojala J, Kaijaluoto S, Jokelainen I and Kosunen A 2016 *J. Appl. Clin. Med. Phys.* **17** 360
[48] Sempau J, Fernàndez-Varea J M, Acosta E and Salvat F 2003 *Nucl. Instrum. Methods Phys. Res.* B **207** 107–23
[49] van Tilborg J, Schroeder C B, Filip C V, Tòth Cs, Geddes C G R, Fubiani G, Huber R, Kaindl R A, Esarey E and Leemans W P 2006 *Phys. Rev. Lett.* **96** 014801
[50] Li W, Li F, Huang Q, Shen J, Wolf F, He Y, Liu X,Hu Y A, Bedford J S and Li C Y 2011 *Cancer Res.* **71** 4130
[51] Löbrich M *et al* 2010 *Cell Cycle* **9** 662
[52] Bonner W M, Redon C E, Dickey J S, Nakamura A J, Sedelnikova O A, Solier S and Pommier Y 2008 *Nat. Rev. Cancer.* **8** 957
[53] Yogo A *et al* 2009 *Appl. Phys. Lett.* **94** 181502
[54] Kraft S D *et al* 2010 *New J. Phys.* **12** 085003
[55] Rigaud O, Fortunel N O, Vaigot P, Cadio E, Martin M T, Lundh O, Faure J, Rechatin C, Malka V and Gauduel Y A 2010 *Cell Death Disease* **1** e73
[56] Cardarelli F, Bizzarri R, Serresi M, Albertazzi L and Beltram F 2009 *J. Biol. Chem.* **284** 36638
[57] Bizzarri R, Cardarelli F, Serresi M and Beltram F 2012 *Anal. Bioanal. Chem.* **403** 2339